A Retrofitting Framework for Pre-Northridge Steel Moment-Frame Buildings

15 WCEE
LISBOA 2012

A. B. Bjornsson & S. Krishnan
California Institute of Technology, United States

SUMMARY:
In this paper, we design and evaluate one retrofit scheme for a pre-Northridge 18-story steel moment-frame building using nonlinear time-history analyses under 3-component synthetic ground motion waveforms at 784 sites in the greater Los Angeles region from the magnitude 7.8 ShakeOut scenario San Andreas earthquake. We realize a reduction of ~23% in the collapse potential of the building. This case study is part of a broader study to construct a rigorous retrofitting framework for this class of existing buildings

Keywords: Moment-Frame, Braced-Frame, Pre-Northridge Connections, ASCE-41-06.

1. INTRODUCTION

In the 1994 magnitude 6.7 Northridge earthquake an unexpected flaw was exposed in steel moment-frame buildings. Field welded-field bolted beam-to-column connections in several buildings experienced brittle fracture, even at low levels of shaking. Prior to this event, the connections were believed to be capable of undergoing large inelastic deformations and were therefore widely utilized in the construction of tall buildings in the 10-30 story range. There is a great deal of uncertainty regarding the number and extent of this localized failure mode in existing buildings in southern California. The costs of potential retrofit schemes and their impact on the architecture are unknown and owners have been reluctant to consider undertaking retrofit measures. Therefore the majority of these buildings have been left unaltered. They may be susceptible to collapse in the event of a major earthquake. In order to reduce the collapse potential of these existing buildings, retrofitting measures must be taken. These measures must realize a lower probability of collapse for the structures at a given intensity of ground shaking when compared to the existing versions. At the same time, they need to be economically feasible and, to the extent possible, must preserve the architectural integrity and functionality of the building.

Rupture-to-rafters simulations offer a convenient platform for exploring possible benefits of a range of retrofit schemes that could be adopted for a given building. These simulations involve the modeling of earthquake sources at one end, numerically propagating the seismic waves through the earth structure, and simulating the impact on engineered structures at the other end using high-performance computing. By generating multiple plausible realizations of large ruptures on the most threatening fault systems in the proximity of the building, computing the response of the retrofit schemes to the resulting ground motions and performing a cost-benefit analysis on a suite of retrofit schemes, we identify the optimal scheme with the greatest reduction in collapse potential for the least cost (including a reduction in lease rate associated with architectural impact).

In recent years, there have been significant advancements in earthquake rupture modeling and seismic wave propagation through the earth's crust into mega cities such as Los Angeles. Examples of such simulations include the magnitude 7.8 ShakeOut scenario on the San Andreas fault, with rupture initiating in Bombay Beach, propagating northwest and terminating in Lake Hughes (Graves et al.

2011), a magnitude 7.9 1857-like San Andreas earthquake with a rupture that initiates in Parkfield, propagates southeast, and terminates in Wrightwood (Krishnan et al. 2006c), and a magnitude 7.2 earthquake on the Puente Hills fault, underneath downtown Los Angeles (Graves et al. 2006).

In order to systematically develop a framework for retrofitting existing pre-Northridge steel moment-frame buildings, we start with a case study of an existing 18-story office building, located within five miles of the epicenter of the Northridge earthquake. It was designed according to the 1982 Uniform Building Code (UBC) and its construction was completed in 1986-87 (SAC 1995, Krishnan et al. 2011). Many moment-frame beam-to-column connections in the building fractured during the Northridge earthquake. We develop thirteen retrofit schemes which involve progressively increasing degrees of intervention using various permutations and combinations of braces in the moment-frame bays and/or stair case core, at every story or at alternate stories, over the full height or half the height of the building. The retrofit schemes are designed to satisfy the basic safety objective (BSO) of ASCE-41-06, Seismic Rehabilitation of Existing Buildings. We analyse FRAME3D models of the existing building as well as the 13 retrofit schemes under 3-component synthetic ground motion waveforms from the ShakeOut scenario and the 1857-like San Andreas earthquakes and the Puente Hills blind-thrust earthquake. We compute the margins against collapse of each model for each record and simultaneously estimate the cost of retrofit. By plotting the median margin against collapse of each scheme against the retrofit cost of the scheme, we can determine the cost-effectiveness of each scheme. Performing such analyses on several index buildings would provide a clear picture of what degree and cost of retrofitting would be required to gain a marginal reduction in collapse potential for this class of buildings. An estimate of the reduction in lease rate associated with the intrusion of the added elements amortized over the building life is folded into the cost of retrofitting. To compute the margin against collapse, all the possible collapse mechanisms for each retrofit scheme are identified. This was recently done by Krishnan and Muto (2011) for the case of steel moment-frame buildings. They demonstrated the existence of a few preferred collapse mechanisms in these buildings and suggest a method to identify these critical mechanisms. In this method, they idealize a sidesway collapse mechanism as a quasi-shear band of stories sandwiched between an upper and a lower set of stories that remain more or less elastic. They compute the critical acceleration of the over-riding block needed to fully plasticize the quasi-shear band (and hence form the collapse mechanism). They show that the preferred collapse mechanism(s) has the lowest critical acceleration. By comparing an estimated level of acceleration of the block overriding the critical quasi-shear band against the critical acceleration, on can estimate the margin against collapse.

In this paper we present one of the conceived retrofit schemes and contrast its performance in the ShakeOut scenario earthquake against the performance of the existing building using the peak transient inter-story drift ratio as a performance measure. These are early results of this ongoing project and future work will involve the methodology described above.

2. THE EXISTING PRE-NORTHRIDGE STEEL MOMENT-FRAME BUILDING AND ONE RETROFIT SCHEME

The existing 18-story office building which is the focal point of this study, is 75.7 m (248’ 4”) high. Typical story height is 3.96 m (13’ 0”) and the first, seventeenth, and penthouse stories are taller. The lateral force-resisting system consists of two-bay welded steel moment-frames, two apiece in either principal direction of the structure as shown in Fig. 2.1a. The location of the north frame one bay inside of the perimeter gives rise to some torsional eccentricity. Many moment-frame beam-column connections in the building fractured during the Northridge earthquake, and the building has been extensively investigated since then by engineering research groups (SAC 1995). An isometric view of its FRAME3D model is shown in Fig. 2.1b. Fundamental periods, computed assuming 100% dead load and 30% live load contribution to the mass, are 4.52s (X-translation), 4.26s (Y-translation) and 2.69s (torsion).

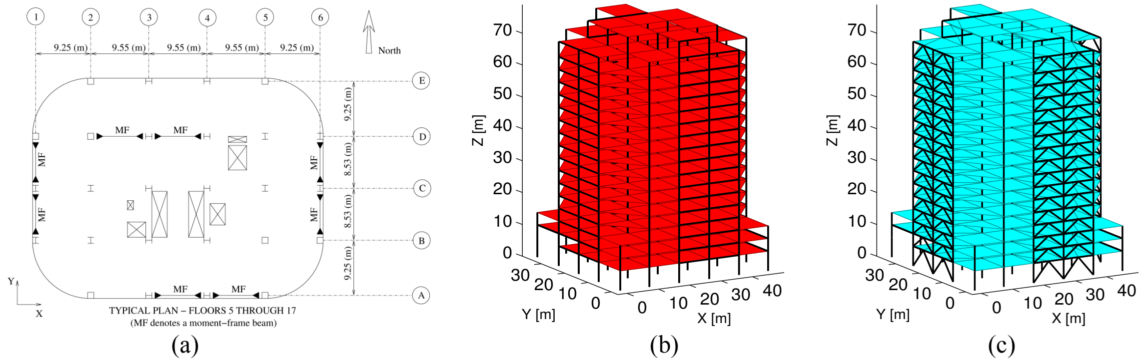

Figure 2.1 (a) Plan view of a typical floor of the existing building, showing the location of columns and moment-frame beams. (b) Isometric view of a FRAME3D finite-element model of the existing building. (c) Isometric view of a FRAME3D finite-element model of the retrofit scheme.

In this study we investigate chevron brace frame systems but other alternatives such as buckling-restrained brace (BRB) systems or systems with viscous fluid dampers or other "added damping and stiffness (ADAS)" devices should be investigated as well. Two locations within the floor plan of the existing building stand out as potential targets for introducing retrofit elements: in the existing moment-frame bays, and in the stair-case core. The significantly larger sizes of the beams and columns in the moment-frames when compared to gravity framing elsewhere makes this a logical target for introducing braces. However, brace elements diminish the available panorama and the impact on the architectural integrity and functionality must be accounted for when evaluating the overall cost of the retrofit scheme. Introducing bracing around the stair case core, on the other hand, leads to minimal architectural impact. But, the surrounding columns, not being part of the lateral-resisting system of the existing building, may need to be strengthened substantially. Furthermore, Krishnan and Muto (2011) identified the preferred collapse mechanisms of the existing building to be located in its lower half. Therefore, we investigate introducing brace elements to the lower half of the building alone. Finally, we investigate the potential benefits of introducing brace elements to every alternate story rather than every story. The resulting structural system effectively results in a strong beam-weak column configuration and generally undesirable. However, adding braces to every alternate story only may reduce P-Δ effects enough to offset the reduction in ductility with column yielding prior to beam yielding. Additionally, strengthening a structure by introducing braces within the existing configuration renders it being much stiffer, thus shifting dynamic character of the structure, generally, to a more energetic regime of earthquake ground motions resulting in greater stiffness forces. Adding braces to every alternate story only may diminish this effect while reducing P-Δ effects. Using permutations and combinations of these retrofit measures we have developed the following 13 retrofit schemes: (i) strengthen beam-column connections; (ii) chevron bracing in every story in the moment frame bays over the bottom half of the building; (iii) chevron bracing in every story in the moment frame bays over the full height; (iv) chevron bracing in every story around the staircase core over the full height; (v) chevron bracing in every story around the staircase core over the full height and in the moment frame bays over the bottom half; (vi) chevron bracing in every story around the staircase core and in the moment frame bays over the full height; (vii) chevron bracing in every story around the staircase core and in the moment frame bays over the bottom half. Schemes (viii)-(xiii) are analogus to schemes (ii)-(vii) except braces are introduced only in every alternate story.

Here, we present results for retrofit scheme (iii) with concentric chevron bracing in the moment frame bays in every story of the structure (Fig. 2.1c). Fundamental periods of this scheme, computed assuming 100% dead load and 30% live load contribution to the mass, are 2.07 s (X-translation), 2.02s (Y-translation) and 1.24s (torsion).

A nonlinear dynamic procedure is used to ensure that the retrofit scheme satisfies the Basic Safety Objective (BSO) as defined in ASCE-41-06, Seismic Rehabilitation of Existing Buildings (ASCE

2007). The BSO rehabilitation objective achieves the dual performance levels of Life Safety (LS) and Collapse Prevention (CP) for the Basic Safety Earthquake-1 (BSE-1) and BSE-2 earthquake hazard levels, respectively. The BSE-1 and BSE-2 earthquake hazard levels essentially refer to seismic hazard levels that have a 10% and 2% probability of exceedance in 50 years, respectively. To obtain fairly conservative, yet representative, seismic loading for design purposes in the Los Angeles greater metropolitan area, we take the maximum considered earthquake (MCE) maps prepared by NEHRP (FEMA 2004), make corrections for site-conditions using the site-condition map prepared by Wills et al. (2006), and sample the resulting short-period and long-period design spectral response acceleration parameters (S_{XS} and S_{X1}, respectively) evenly over the region of interest. Then, for design purposes, S_{XS} and S_{X1} are taken as the expected values plus one standard deviation (STD) of log normal probability density function (PDF) fits to the two datasets. The values for the greater Los Angeles area are 2.09 *g* and 1.07 *g*, respectively, where *g* refers to acceleration due to gravity. Maps for S_{XS} and S_{X1}, and histograms of the sampled values overlaid by the log normal PDFs are presented in Fig. 2.2 and Fig. 2.3, respectively. The locations where S_{XS} and S_{X1} are sampled are shown as white triangles.

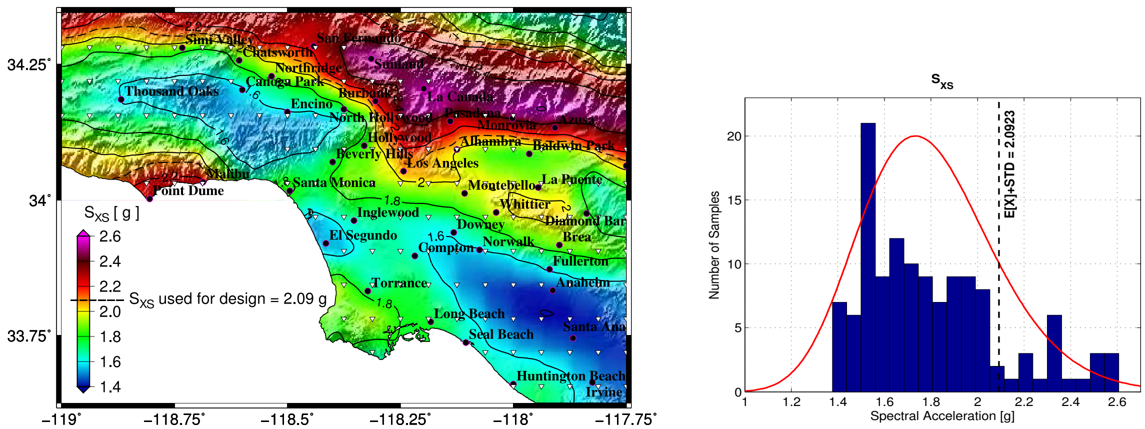

(a) (b)

Figure 2.2 (a) Map for the short-period period spectral response acceleration parameter, S_{XS}, in the region of interest. The locations where S_{XS} is sampled are shown as white triangles. (b) Histogram of the S_{XS} samples overlaid with a log normal PDF fit to the data set. For design purposes, S_{XS} is taken to be the expected value plus one standard deviation (STD) of the log normal PDF (black dashed line).

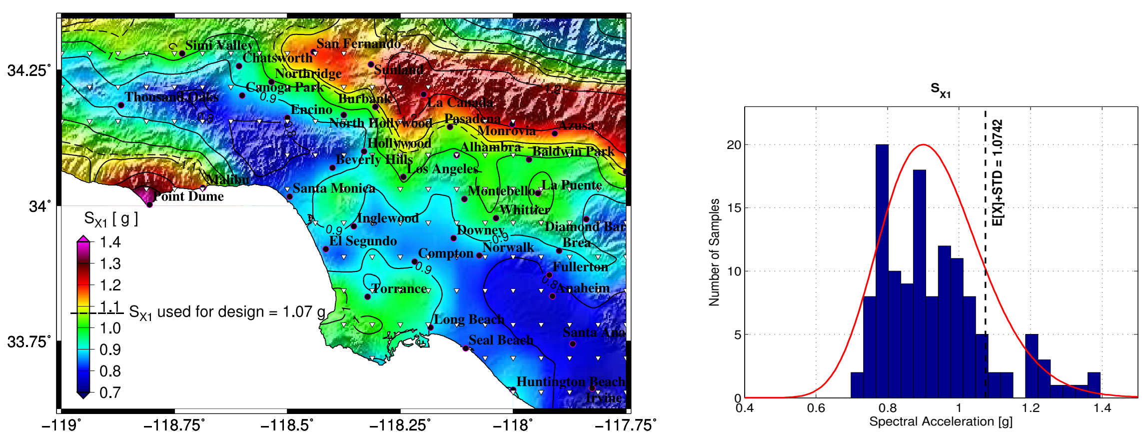

(a) (b)

Figure 2.3 (a) Map for the long-period period spectral response acceleration parameter, S_{X1}, in the region of interest. The locations where S_{X1} is sampled are shown as white triangles. (b) Histogram of the S_{X1} samples overlaid with a log normal PDF fit to the data set. For design purposes, S_{X1} is taken to be the expected value plus one standard deviation (STD) of the log normal PDF (black dashed line).

From the selected S_{XS} and S_{X1} values, a 5%-damped design response spectrum, corresponding to the BSE-2 earthquake hazard level, is derived. A set of seven ground motion records are selected from the PEER database. For each record a square root of the sum of the squares (SRSS) 5%-damped response spectra is constructed from the horizontal components. The records are then scaled such that the average of the seven SRSS response spectra does not fall below 1.3 times the design response spectrum for periods 0.2T and 1.5T (where T is the fundamental period of the building model). This is repeated for BSE-1 earthquake hazard level. The BSE-1 design spectrum is BSE-2 spectrum scaled down by a factor of 2/3. The building model is then subjected to the scaled ground motions with the normal component of the ground motion record (usually the dominant component) along the x-axis of the building model and again with the normal component in the direction of the y-axis. The braces and the plates added to strengthen the columns are sized such that the average peak response of each response parameter in the seven records (for both orientations) is less than the limits required to achieve the Basic Safety Objective (BSO) for the two seismic hazard levels. The SRSS spectra for the ground motion records selected for the existing building and the retrofit scheme, scaled suitably to fit the BSE-2 earthquake hazard level, are shown in Fig. 2.4 a and b, respectively (dashed lines). The average of the seven is shown with a solid red line. The BSE-2 design response spectrum scaled by a factor of 1.3 is shown with a solid black line. The earthquake and seismic station names and scaling factors of the ground motion records are listed in the figure as well. The average peak base shear for retrofit scheme (iii) in the direction of the strong component of the BSE-1 time histories in the two orientations is 0.24 and 0.25 of the seismic weight of the building, respectively. In comparison with that of the existing building (0.09 and 0.11 of the seismic weight, respectively), the average base shear for the retrofit scheme is more than doubled. Such comparison cannot be made at BSE-2 seismic hazard level because collapse of the existing building is simulated before the end of the ground motion record in several records. The seismic weight of the existing building model is taken to be equal to the total dead load (118,345 kN or 26605 kips). This compares well with the seismic weight computed by other research groups (Carlson 1999, Chi et al. 1996, SAC 1995). The weight of added steel in retrofit scheme (iii) is 1.9 percent of the seismic weight of the existing building.

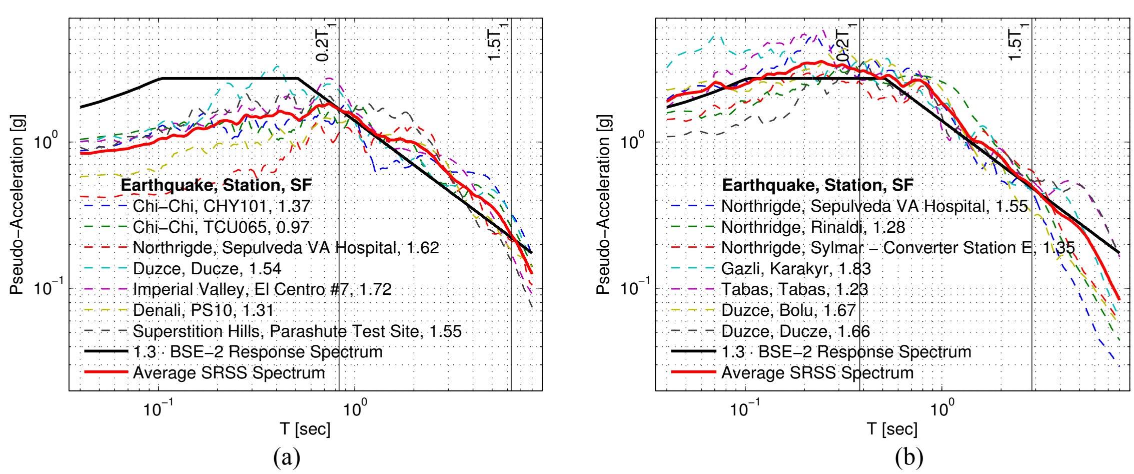

Figure 2.4 Response spectra for the 7 ground motion records selected for the existing building (a) and retrofit scheme (iii), scaled accordingly to fit to the BSE-2 seismic hazard level.

3. FEM MODELING USING FRAME3D

Nonlinear damage analyses of the building are performed using the program FRAME3D (http://virtualshaker.caltech.edu), which has been extensively validated against analytical solutions of simple problems and cyclic data from component tests, as well as pseudodynamic full-scale tests of assembled structures (Krishnan 2009a, 2009b, 2010). FRAME3D incorporates material and geometric nonlinearity, which enables the modeling of the global stability of the building, accounting for P-Δ effects accurately. Here, beams are modeled using segmented elastofiber (EF) elements, with nonlinear end segments that are subdivided in the cross section into a number of fibers, and an interior elastic segment, as shown in Fig. 3.1. The stress-strain response of each fiber in the nonlinear end-segments is hysteretic, including flexural yielding, strain-hardening and ultimately rupture of the fiber. The hysteretic rules that define the cyclic response of each fiber are given by Challa (1992). Since strength and stiffness of the element end segments are integrals of the corresponding quantities over all the fibers comprising the segment, they too can degrade as the stresses in the fibers exceed the ultimate stress and traverse the downhill path to rupture. In the extreme event that all the fibers of a fiber segment rupture, there will be a complete severing of the element. In addition, a fiber fracture capability, in the form of a general probabilistic description of the fracture strain, is available to approximately represent fracture of welded beam-to-column connections (Hall et al. 1995, Krishnan 2009b). When the fiber strain reaches the fracture strain, it fractures and can no longer take tension, but, upon reversal of loading the fractured and separated parts can come in contact, and the fiber is able to resist compression again. Columns and braces are modeled using modified elastofiber (MEF) elements which are similar to the EF element but contain an additional fiber segment at mid-span. The nonlinear middle segment can be given an initial out-of-plane offset to mimic element imperfections. The additional fiber segment enables the element to accurately capture out-of-plane buckling of braces and slender columns (Krishnan 2009a, 2010). Beam-to-column joints are modeled in three dimensions using panel zone elements that include shear yielding. These elements have been shown to simulate damage accurately and efficiently (Krishnan et al 2006a, 2006b). Lastly, in-plane stiffness of floor and roof slabs is modeled using plane-stress elements that remain elastic at all times. Story masses are lumped at column locations based on plan tributary area. A rigid foundation is assumed, with the base of all columns fixed.

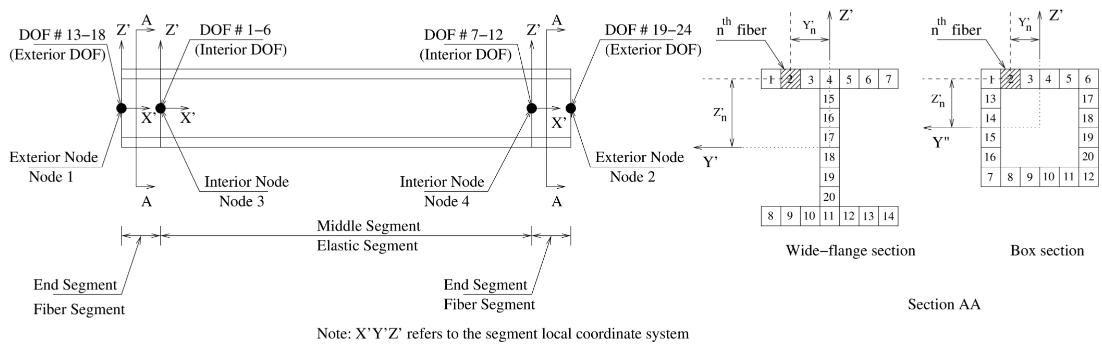

Figure 3.1 Schematic representation of the elastofiber (EF) element used to model beams. Each element is divided into a linear elastic middle segment and two nonlinear end fiber segments. The fiber segments are comprised of 20 nonlinear fibers that run the length of the segment (section view A-A).

To model fracture in moment connections, we utilise the fiber fracture capability of EF and MEF elements in FRAME3D. Since there were significantly greater number of fractures observed in the bottom flanges of beams during the Northridge earthquake, a more susceptible probability distribution is assumed for the fibers in the beam bottom flange when compared against that assumed for the fibers in the top flange and the web. For the fibers in the bottom flanges of moment frame beams, represented by fibers 8 to 14 in Fig. 3.1, probability is 20% that the fracture strain is 0.9 times the yield strain, ε_y; 20% that it is 2 ε_y; 20% that is 5 ε_y; 20% that is 15 ε_y; and 20% that it is 40 ε_y. For the top-flanges, represented by fibers 1-7 in Fig. 3.1, and the webs of the beams, represented by fibers 15-20 in the figure, probability is 30% probability that the fracture strain is 10 ε_y; 30% that it is 20 ε_y; 20% that it is 40 ε_y; and 20% that it is 80 ε_y. At each connection, the fracture strain in all the beam bottom flange fibers is taken to be a random variable. At the beginning of the time-history analysis, a single realization of this random variable is generated from the corresponding distribution and assigned to the fracture strain of all the beam bottom flange fibers at a given connection. This is repeated for the bottom flange fibers as well as the web and the top flange fibers at either segment of each beam. For column flange and web fibers, fracture strain is drawn from the same distribution as for the beam web and top flange fibers. Brace element fiber fracture strain is assumed to be far greater than the rupture strain, thus precluding the occurrence of fractures.

This fiber fracture strain statistical distribution was first proposed by Hall (1998) based on the performance of steel beam-column moment connections in existing buildings during the Northridge earthquake. It also compares reasonably well with experiments performed following the Northridge earthquake and documented in FEMA 355d, "A State of the Art Report on Connection Performance (FEMA 2000)". Based on the test data, FEMA 355d relates the mean (μ_{θ_p}) and standard deviation (σ_{θ_p}) of the connection plastic rotation (in radians) at which fracture is observed to the beam depth (in inches) for older pre-Northridge connections, welded with E70T-4 electrode and with steels with lower yield to tensile stress ratios (Eqn. 3.1), and more recent pre-Northridge connections, welded with E70T-4 electrode and with steels with larger yield to tensile stress ratios (Eqn. 3.2):

$$\mu_{\theta_p} = 0.051 - 0.0013d \quad \& \quad \sigma_{\theta_p} = 0.0044 + 0.0002d \tag{3.1}$$

$$\mu_{\theta_p} = 0.011 \quad \& \quad \sigma_{\theta_p} = 0.007 \tag{3.2}$$

In these equations, d is the beam depth in inches. To compare the connection behavior resulting from the proposed fiber fracture strain statistical distribution to the experimental results, we construct FRAME3D models of three typical beam-column sub-assemblies from the existing building and apply the SAC connection testing loading protocol (SAC 1997) to these models. Four hundred realizations are produced for each model. A histogram of the plastic rotation at the first instance of fracture in the models is shown in Fig. 3.2. A log-normal fit to the histogram is also shown. The corresponding log normal PDFs for older pre-Northridge connections (cyan line) and more recent pre-Northridge connections (magenta line), derived using Eqns. 3.1 and 3.2, respectively, are also shown for comparison. The PDF of θ_p at fracture from the Hall distribution lies between that estimated by FEAM for older pre-Northridge and newer pre-Northridge connections, confirming that the Hall distribution is a reasonable characterization of fracture strains in pre-Northridge connections.

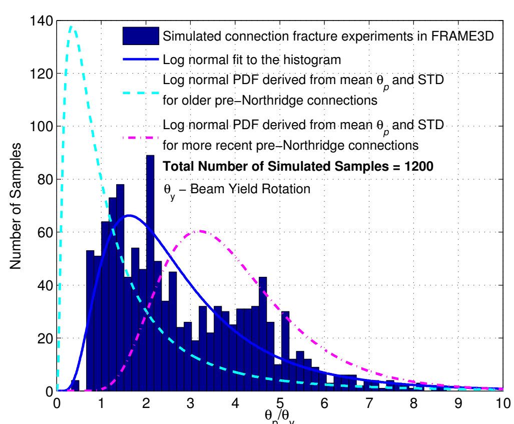

Figure 3.2 Distribution of connection (beam end) plastic rotation at which initial fracture occurs or when moment resistance drops below 80% of the initial plastic moment capacity.

As with any modeling techniques there are some limitations inherent in the FRAME3D models that need to be mentioned. Local buckling of I-section flanges and low-cycle fatigue are not included in the modeling of the beam/column/brace elements. The FRAME3D models also do not include column splices, composite action due to the connection between moment-frame beams and floor slabs, damage to floor slabs, stiffness of partitions, and staircase and elevator enclosures, structure foundations, and soil-structure interactions. We include gravity bearing columns, but preclude gravity bearing beams.

4. ANALYSIS OF BUILDING PERFORMANCE UNDER THE MAGNITUDE 7.8 SAN ANDREAS FAULT SHAKEOUT SCENARIO EARTHQUAKE

The hypothetical M_w 7.8 ShakeOut scenario earthquake on the southern part of the San Andreas fault initiates at Bombay Beach and propagates 305 km north along the fault, and terminates at Lake Hughes near Palmdale as shown in the inset of Fig. 4.1. 3-component broadband ground motion time-histories, obtained at 784 sites evenly distributed in the greater Los Angeles region, are used to analyze the existing building and the retrofit scheme, hypothetically located at each site. The sites are shown as triangles in Fig. 4.1. The broadband (0 – 10 Hz) ground motion simulations use a hybrid procedure, combining a 3D deterministic approach at low frequencies (<1 Hz) with a semi-stochastic approach at high frequencies (> 1Hz) (Graves 2008, 2011). Peak ground velocities (PGV) realized in the earthquake scenario are shown for E-W and N-S directions in Fig. 4.2. Peak ground velocities are in the range of 0-1 m/s in the San Fernando Valley, 0.6-1.5 m/s in the Los Angeles basin, and from 0.5 m/s-2.0m/s in the San Gabriel Valley. Building performance is evaluated and compared based on simulated peak transient inter-story drift ratio (IDR). ASCE-41-06 sets forth IDR exceedance limits for the Immediate Occupancy (IO), Life Safety (LS), and Collapse Prevention (CP) performance levels. For steel moment-frame buildings these limits are 0.007, 0.025 and 0.05, respectively, and for steel braced-frame buildings these limits are 0.005, 0.015, and 0.02, respectively (ASCE 2007). The retrofit scheme shows substantial improvement in structural performance at most locations when compared against the existing building performance based on peak transient IDR values (Fig.4.3). Through the retrofit, we reduce the cumulative probability of exceeding the IO, LS and CP performance levels at PGV levels of 1 m/s by 4.1, 30.0 and 23.3 percent, respectively (Fig.4.4).

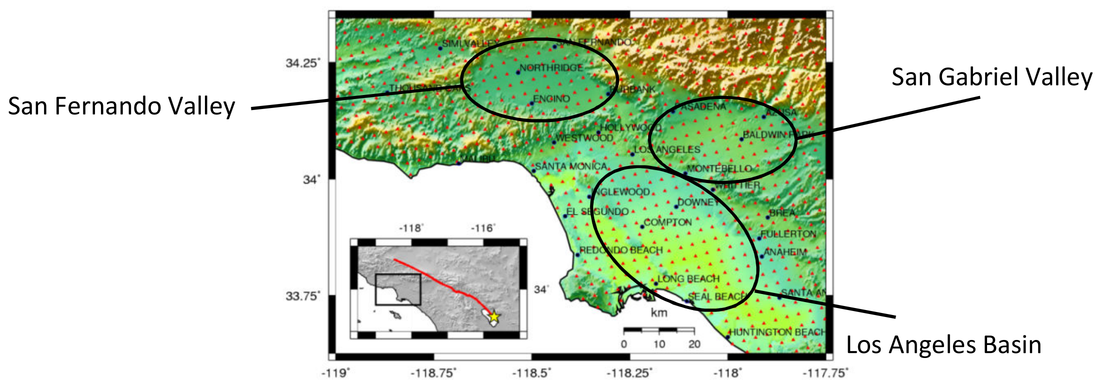

Figure 4.1 Geographical scope of the study area. Triangles represent sites where the building time-history analyses are performed. The inset shows the study area in relation to the rupture trace. The star represents the epicentre of the earthquake.

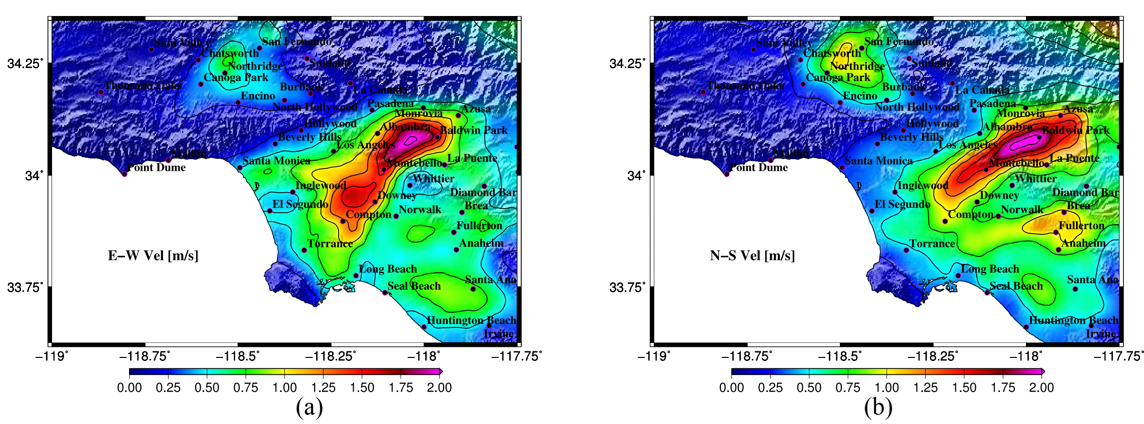

Figure 4.2 Peak ground velocities (in m/s) realized in the magnitude 7.8 San Andreas fault ShakeOut earthquake scenario in (a) E-W and (b) N-S directions.

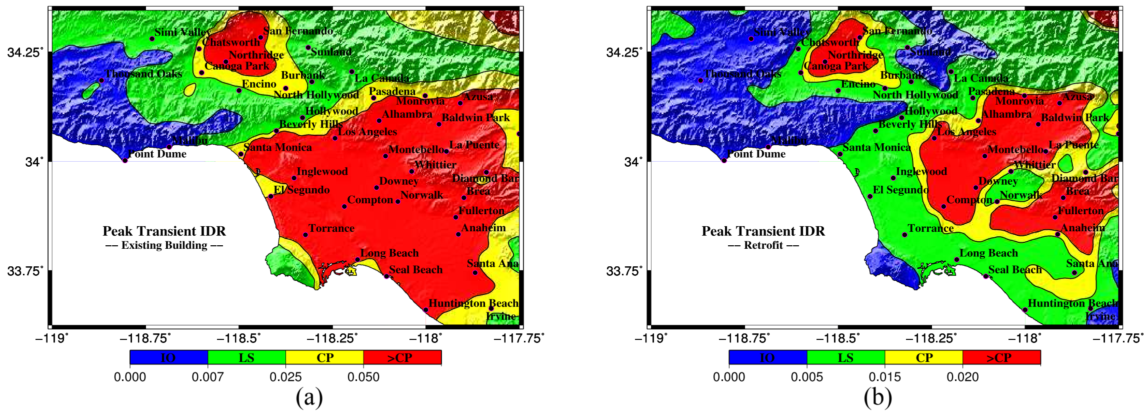

Figure 4.3 Simulated peak transient IDR in (a) the existing building and (b) the retrofit scheme, under 3-component ground motion from the magnitude 7.8 ShakeOut scenario earthquake.

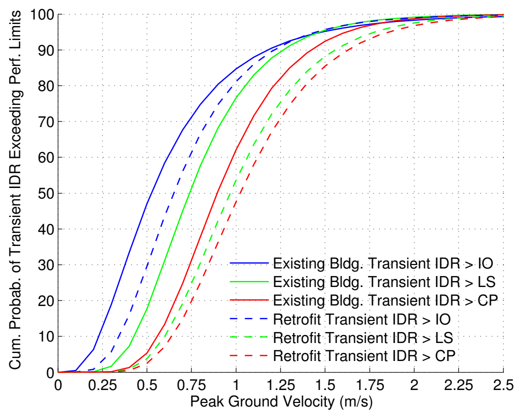

Figure 4.4 Cumulative probability of the peak transient IDR exceeding the ASCE-41-06 IO, LS, and CP performance levels, given PGV of shaking in the greater Los Angeles region from the magnitude 7.8 ShakeOut scenario earthquake.

5. CONCLUSIONS

In this paper the initial steps of a more extensive body of work currently being undertaken are presented. The ultimate goal of this body of work is to establish a retrofitting framework for pre-Northridge steel moment-frame buildings. To achieve this goal we are developing 13 retrofit schemes for an existing steel moment-frame building that was built before the Northridge earthquake and contains moment connections susceptible to failure. The performance of these schemes under synthetic ground motion in the greater Los Angeles region from the magnitude 7.8 ShakeOut scenario San Andreas earthquake, the magnitude 7.9 1857-like San Andreas earthquake, and the magnitude 7.2 Puente Hills fault earthquake are being compared against that of the existing building. Preliminary results presented here are promising, with collapse probability being reduced by ~23% using one example retrofit scheme under the ShakeOut scenario earthquake.

AKCNOWLEDGEMENT
We are grateful to Rob Graves of the United States Geological Survey (USGS) for providing us with the ground motion waveforms from the ShakeOut Scenario earthquake. This work is funded in part by USGS.

REFERENCES

American Society of Cvil Engineers (ASCE) (2007). Seismic Rehabilitation of Existing Buildings. ASCE Standard ASCE/SEI 41-06. ASCE, Reston, Virginia, USA

Chi, W.-M., El-Tawil, S., Deierlein, G.G., and Abel, J.F. (1996). Inelastic Analyses of a 17 Story Steel Framed Building Damaged During Northridge. Engineering Structures. **20:4-6**, 481-495.

Carlson, A. (1999). Three-dimensional nonlinear analysis of tall irregular steel buildings subject to strong ground motion. Technical Report EERL 99-02, Earthquake Engineering Research Labaratory, California Institute of Technology, Pasadena, CA, USA.

Challa, V. R. M. (1992). Nonlinear seismic behavior of steel planar moment-resisting frames. Tehcnical Report EERL 92-01, Earthquake Engineerling Laboratory, California Institute of Technology, Pasadena, CA, USA.

FEMA (2000). A State of the Art Report on Connection Performance. FEAM 355d, Federal Emergency Management Agency, Washington, D.C., USA

FEMA (2004). NEHRP recommended provisions for seismic regulations for new buildings and other structures, 2003 Ed. – Part 1: Provisions and Part 2: Commentary. FEMA 450 and FEMA 451, prepared by the Building Seismic Safety Council for the Federal Emergency Management Agency, Washington, D.C., USA

Graves, R., Aagaard, B., Hudnut, K., Star, L., Stewart, J., and Jordan, T. (2008). Broadband simulation for Mw 7.8 souther San Andreas earthquakes: Ground motion sensitivity to rupture speed. *Geophysical Research Letters,* **35**, L22302, soi:10.1029/2008GL035750.

Graves, R., Aagaard, B., and Hudnut, K. (2011). The ShakeOut earthquake source and ground motion simulations. *Earthquake Spectra.* **127**, 273-291.

Graves, R., and Somerville, P. (2006). Broadband Ground Motion Simulations for Scenario Ruptures of the Puente Hills Fault. *Proceedings of the 8th U.S. National Conference on Earthquake Engineering.* Paper no. 1052.

Hall, J. F., and Challa, V. R. M. (1995). Beam-column modeling. *Journal of Engineering Mechanics.* **121:12**, 1284-1291.

Hall, J. F. (1998). Seismic response of steel frame buildings to near-source ground motions. *Earthquake Engineering and Structural Dynamics.* **27,** 1445-1464.

Krishnan, S. (2009a). On the Modeling of Elastic and Inelastic, Critical and Post-Buckling Behavior of Slender Column and Bracing Members. Technical Report **Caltech EERL-2009-03**, California Institute of Technology, Pasadena, California, USA

Krishnan, S. (2009b). FRAME3D 2.0 – A Program for Three-Dimensional Nonlinear Time-History Analysis of Steel Buildings: User Guide. Technical Report **Caltech EERL-2009-04**, California Institute of Technology, Pasadena, California, USA

Krishnan, S. (2010). The modified elastofiber element for steel slender column and brace modeling. *Journal of Structural Engineering.* **136**, 1350-1366.

Krishnan, S. and Hall, J. F. (2006a). Modeling of Steel Frame Buildings in Three Dimensions – Part I: Panel Zone and Plastic Hinge Elements and Examples. *Journal of Engineering Mechanics.* **132**, 345-358.

Krishnan, S. and Hall, J. F. (2006b). Modeling of Steel Frame Buildings in Three Dimensions – Part II: Elastofiber Beam Element And Examples. *Journal of Engineering Mechanics.* **132**, 359-374.

Krishnan, S., Ji, C., Komatitsch, D., and Tromp, Ju. (2006c). Performance of Two 18-Story Steel Moment-Frame Buildings in Souther California During Two Large Simulated San Andreas Earthquakes. *Earthquake Spectra.* **22:4**, 1035-1061.

Krishnan, S., and Muto, M. (2011). Mechanism of collapse of tall steel moment-frame buildings under earthquake excitation. *Journal of Structural Engineering*.

SAC (1995). Analytical and Field Investigations of Buildings Affected by the Northridge Earthquake of January 17, 1994 – Part 2: Tech. Rep. SAC 95-04, Part 2, Structural Engineers Association of California, Applied Technology Council and California Universities for Research in Earthquake Engineering, Sacramento, CA, USA

SAC (1997). Protocol for Fabrication, Inspection, Testing, and Documentation of Beam-Column Connection Tests and Other Experimental Specimens Rep. SAC/BD-97/02, Structural Engineers Association of California Applied Technology Council and California Universities for Research in Earthquake Engineering, Sacramento, CA, USA